Primary Angle-Closure Glaucoma: A Comprehensive Meta-Narrative Review — Part 2

Derek MacDonald, OD, FAAO, Dipl AAO
Optometrist, Ilex Eyecare
Waterloo, Ontario, Canada

Abstract

Primary angle-closure glaucoma, while less common than primary open-angle glaucoma, carries a 4- to 5-fold greater risk of severe visual morbidity. The identification of individuals at high risk of the disease enables proactive rather than reactive intervention, which helps mitigate the possibility of potentially serious consequences. Recognition is facilitated by careful case history, clinical examination, and ancillary imaging, while management is an evolving paradigm, informed by numerous relatively recent investigations, that may involve medications, laser procedures, surgery, or a combination thereof. This series of 4 papers, drawing upon relevant peer-reviewed literature, will endeavour to provide a comprehensive yet focused synthesis and synopsis of the contemporary diagnosis and management of primary angle-closure glaucoma. This part will deal with ancillary imaging modalities, including anterior segment optical coherence tomography and quantitative anterior segment parameters.

Keywords

primary angle-closure glaucoma, gonioscopy, anterior segment optical coherence tomography, pupillary block, plateau iris, angle-closure continuum, laser peripheral iridotomy, cataract extraction

Qualitative Ancillary Imaging Modalities: Photography

Documentation of angle status, much like documentation of optic nerve head status, can be facilitated by photography. Slit lamp photography can provide incredibly high-resolution colour images of the anterior segment but is technically challenging and time consuming to perform.

Suggested citation

MacDonald D. Primary Angle-Closure Glaucoma: A Comprehensive Meta-Narrative Review — Part 2. *Can J Optom.* 2026;88(2):13-26.
https://www.doi.org/10.65636/cjo.v88i2.6758

Automated software-driven 360° angle photodocumentation is one means to address this barrier. An instrument with a 16-mirror indirect gonioscope lens can be used to capture sixteen 22.5° (2.0 × 2.36 mm) high-resolution colour photographs. Each image is captured in 17 different planes to account for variations in angle depth, with the most in-focus used for analysis. These images may be reviewed individually, or because they do overlap slightly, combined in a circular or linear montage.[1] While not a replacement for traditional gonioscopy (being static, 2-dimensional, and not allowing for dynamic or compression/indentation techniques), this standardized approach can assist in documentation, facilitate comparison between quadrants, allow off-line as opposed to only real-time analysis, and enable detection of change over time, including post-treatment, through the longitudinal evaluation of serial images.[2,3]

Quantitative Ancillary Imaging Modalities

Highly reproducible quantitative information can be a helpful adjunct to qualitative gonioscopic assessment, perhaps particularly in predicting risk of progression.[4] However, gonioscopy remains invaluable in identifying important features, including peripheral anterior synechiae (PAS), which can be difficult to detect with current imaging modalities.[5,6]

Ancillary imaging procedures — including ultrasound biomicroscopy, Scheimpflug imaging, and most recently, anterior segment optical coherence tomography — have identified numerous novel biometric parameters that are risk factors for angle closure.[7-9] Like gonioscopy, control of fixation, illumination, accommodation, and lid position are critical to maintain globe position and prevent pupillary constriction, allowing representative anterior segment images to be obtained.[5,10]

Abbreviation List

ACA	anterior chamber area
ACD	anterior chamber depth
ACV	anterior chamber volume
AOD	angle opening distance
AOD_{SL}	angle opening distance at the level of Schwalbe's line
APAC	acute primary angle closure
ARA	angle recess area
AS-OCT	anterior segment optical coherence tomography
CB	ciliary body
IC	iris curvature
ITC	irido-trabecular contact
LPI	laser peripheral iridotomy
LV	lens vault
PAC	primary angle closure
PACG	primary angle-closure glaucoma
PACS	primary angle-closure suspect
PAS	peripheral anterior synechiae
SL	Schwalbe's line
SD-OCT	spectral domain optical coherence tomography
SS	scleral spur
TIA	trabecular-iris angle
TISA	trabecular-iris space area
$TISA_{LS}$	trabecular-iris space area at the level of Schwalbe's line
TM	trabecular meshwork
UBM	ultrasound biomicroscopy

Ultrasound Biomicroscopy

Ultrasound biomicroscopy (UBM), introduced in the late 1980s, is a non-invasive, 2-dimensional imaging technique based on the reflection of focused high-frequency (most commonly 50 MHz) sound waves from tissues of different impedances.[11]

UBM provides axial and lateral resolution of 25 µm and 50 µm, respectively, and tissue penetration of 3 to 5 mm.[12] Penetration may be improved with the use of lower frequencies, albeit at the expense of poorer resolution. In fact, one of the greatest strengths of UBM is its ability to penetrate the iris pigment epithelium and image the ciliary body (CB), which is of particular value in cases of plateau iris (to be reviewed in more detail later in this series).[2,11,12]

UBM can accurately identify narrow angles and detects irido-trabecular contact (ITC) more often than gonioscopy.[13,14]

UBM was the first modality to quantify parameters, including anterior chamber depth (ACD), angle opening distance (AOD), and angle recess area (ARA), among others. Many of these metrics will be detailed in the review of anterior segment optical coherence tomography (AS-OCT) to follow.[12,15]

By virtue of its ability to image structures posterior to the iris, UBM is also able to quantify parameters not possible with AS-OCT, including trabecular-ciliary process distance and trabecular-ciliary process angle, both of which are smaller in the presence of an anteriorly positioned CB that characterizes plateau iris.[16]

Figure 1. A swept-source anterior segment optical coherence tomography image depicting the localization of the nasal and temporal scleral spur (red arrows) and nasal and temporal Schwalbe's line (blue arrows).

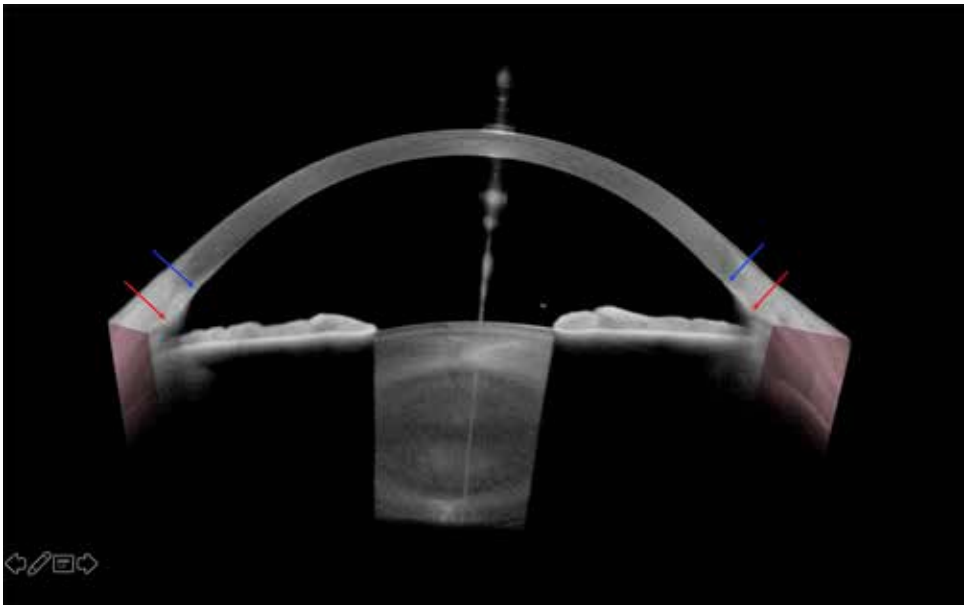

The scleral spur is characterized by a subtle change of curvature (or bump) marking the insertion of the ciliary muscle about 500 µm posterior to the trabecular meshwork. Schwalbe's line marks the peripheral termination of Descemet's membrane, lying between the anterior trabecular meshwork and the corneal endothelium.

Pre- and post-laser peripheral iridotomy (LPI) UBM images are able to demonstrate an increase in AOD and ARA, and a decrease in iris convexity due to the successful elimination of pupillary block.[17] However, patients must be supine to allow the ultrasound probe to be immersed in a pre-corneal water bath and fixate on a distant target with the fellow eye to control accommodation. Ambient illumination must be low to control pupil size.[13] Moreover, inter-examiner repeatability can be problematic due to inconsistency in probe positioning and manual identification of important anatomic landmarks, most often the scleral spur (SS).[2]

Scheimpflug Imaging

In conventional photography, the planes of the lens, film, and focus are parallel. In Scheimpflug imaging, tilting the plane of the lens to intersect the other 2 planes extends depth of focus, allowing simultaneous imaging of structures between the anterior cornea and posterior lens.[18] The prototypical Pentacam instrument uses a 475 nm light source and rotating Scheimpflug camera to acquire multiple cross-sectional photographs and generate a 3-dimensional model of the anterior segment.[19,20]

Scheimpflug imaging is able to quantify ACD and anterior chamber volume (ACV) and their change post-LPI or post-lens extraction, but does not allow for direct visualization of the angle and is subject to the influence of accommodation and lighting.[2,12] Moreover, it tends to show poor correlation with gonioscopy, particularly in narrow angles. Unlike UBM, it is not able to image structures posterior to the iris.[21]

Anterior Segment Optical Coherence Tomography

AS-OCT uses low-coherence near-infrared interferometry to produce cross-sectional in vivo images, allowing both qualitative and quantitative analyses.[22]

Like gonioscopy, it is influenced by ambient lighting and accommodation.[23] Unlike gonioscopy, there is little or no influence of inadvertent mechanical pressure but also no ability to easily perform compression/indentation.[24,25] However, synechial and appositional angle closure may be differentiated through dynamic imaging in light and dark conditions (an angle with PAS will remain closed regardless of ambient illumination), and swept-source AS-OCT is able to detect PAS with a high level of agreement with gonioscopy.[26] Although a horizontal scan is the most easily acquired and most frequently analyzed, clinicians must be cognizant that scans along vertical or oblique axes (akin to gonioscopic examination of multiple quadrants) may yield dramatically different and more representative results.[27-29]

Despite affording already-impressive and ever-improving scan resolution, width, and depth, none of the AS-OCT modalities are currently able to image structures posterior to the iris (or through media opacities) as well as UBM.[12,30,31] However, AS-OCT is more user- and patient-friendly than UBM and provides better repeatability and higher resolution, particularly when multiple images are sampled and averaged.[12,32] This allows more accurate and precise identification of the SS, visualized as a subtle change of curvature (or bump) marking the extension of the brighter sclera (visible anterior to the darker ciliary muscle) into the anterior chamber at its junction with the posterior cornea (refer to Figure 1).[33] The SS is a critical landmark, given that the trabecular meshwork (TM) is found about 500 µm anterior to it.[10,32]

The prototypical 1,310 nm Zeiss Visante time domain AS-OCT provides scan width of up to 16 mm (with 256 A-scans), depth of 8 mm, speed of about 2,000 A-scans per second, and axial and transverse resolution of about 18 µm and 60 µm, respectively.[20]

SS identification can be challenging with time domain AS-OCT, with about 1 in 4 being indeterminate, even when high-quality images are judged by glaucoma specialists with an interest in angle closure.[10,34,35] The challenge can be even greater with the shorter wavelengths (~840 nm) and decreased penetration (~2 mm) and width (~3 mm) of spectral domain OCT (SD-OCT) (a device more commonly used in private practice), particularly in eyes of individuals over the age of 65 years, in the superior and inferior quadrants, and in the presence of any limbal opacity overlying a narrow angle.[32,36-38] This may be even more problematic if images of poorer quality are assessed by practitioners with less experience. Moreover, the inter-observer standard deviation in SS localization can approach 100 µm, introducing significant variability.[2] However, the higher scan speed (from 27,000 to 100,000 A-scans per second) and greater resolution of SD-OCT allows identification of more anterior structures, including TM, Schlemm's canal, and Schwalbe's line (SL).[12,39,40]

Swept-source AS-OCT using a tunable 1,310 nm scanning laser provides scan width and depth (16 mm and 6 to 14 mm, respectively) that rivals dedicated time domain AS-OCT, and speed (30,000 to 200,000 A-scans per second) and axial and transverse resolution (5 to 9 µm and 15 to 30 µm, respectively) that exceeds it.[41-43] Increased scan penetration allows for visualization of the posterior surface of the crystalline lens and calculation of lens thickness, although UBM is still superior in visualizing the CB.[44,45] High-speed image acquisition (scanning 360° in less than 3 seconds) permits simultaneous localization of both SS and SL (representing the posterior and anterior boundaries of the TM), and reconstruction of an impressively detailed 3-dimensional image of the iris and angle structures, allowing the area and angular subtense of PAS to be accurately and precisely quantified, something that is virtually impossible with compression/indentation gonioscopy.[35,46]

AS-OCT Versus Gonioscopy

Early comparisons suggested that both UBM and AS-OCT were strongly correlated with gonioscopic angle grade.[35] However, others demonstrated that AS-OCT detects 50% more appositional closure (defined as any ITC anterior to the SS) than gonioscopy, perhaps by virtue of better control of illumination and less physical manipulation of the globe.[47,48] AS-OCT may also better characterize anatomic variations between quadrants.[49] It was subsequently noted that about 15% of eyes may be falsely categorized as having angle closure (using gonioscopy as the reference standard) when ≥180°

ITC is detected using swept-source AS-OCT.[50] Many of these false-positives had short ITC involving only a portion of the TM. However, eyes with more extensive AS-OCT-detected ITC at baseline do have a greater risk of developing gonioscopically detected angle closure over 4 years of follow-up.[51]

A recent study demonstrated that only 1 in 3 eyes with gonioscopic angle closure (defined as inability to visualize posterior TM ≥180°) had ITC ≥180° on swept-source AS-OCT, and 1 in 6 had absolutely no evidence of ITC at all.[52] This suggests that gonioscopic angle closure may not always represent true anatomic angle closure (that is, posterior TM may not be visible but remains unobstructed) and highlights the potential role of AS-OCT in risk stratification.

As has often proven to be the case in the world of glaucoma (both open angle and angle closure), it is not a question of one technique **or** another, it is one technique **and** another.

AS-OCT Quantified Anterior Chamber Parameters

AS-OCT has identified or refined numerous novel quantitative parameters associated with an increased risk of angle closure, most still hinging on accurate subjective identification of the SS.[10,11,32,53]

A smaller anterior chamber width (ACW) (defined as the horizontal SS-to-SS distance, measured in millimetres) is a risk factor for and a common finding in eyes that are more susceptible to primary angle-closure glaucoma (PACG), including those of women, Chinese individuals, and individuals over the age of 65 years.[35,54]

Mean anterior chamber area (ACA) and anterior chamber volume (ACV) were found to be smaller in eyes with narrow anterior chamber angles and larger following LPI.[53,55] ACA is defined as the cross-sectional area encompassed by the corneal endothelium, anterior iris, and anterior lens in the pupil, measured in square millimetres. ACV is calculated by mathematically rotating the ACA one full rotation around an axis through its midpoint, measured in cubic millimetres.

Both ACD and ACV decrease with age, which may play a role in the pathogenesis of angle-closure disease. Between the ages of 20 and 80 years, average ACD decreases from 3.2 ±0.3 mm to 2.5 ±0.4 mm, and ACV from 2.32 ±0.46 mm^3 to 1.52 ±0.45 mm^3.[56,57] That being said, not all eyes with shallow central ACD have an equivalent risk of developing primary angle-closure disease. In some eyes, the peripheral angle anatomy may be more normal than the central ACD suggests, putting them at relatively low risk of angle closure.[29]

Smaller ACW, ACA, and ACV contribute to anterior segment crowding and increase the risk of incident angle-closure disease.[7] In fact, smaller ACA and ACV increase the odds of having a narrow angle by 40- to 50-fold.[55,57,58]

First quantified by Pavlin in UBM studies, AOD is defined as the length of a line between the anterior iris surface and corneal endothelium, perpendicular to the plane of the TM, at a fixed distance (often 500 or 750 µm) from the SS that is felt to correspond to the location of the TM.[11] AOD is known to be smaller in individuals who progress from primary angle-closure suspect (PACS) to primary angle closure (PAC), is predictive of incident gonioscopic angle closure, and increases following LPI.[6,53] In fact, horizontal AOD_{750} may be the best single parameter to detect gonioscopically narrow angles. A baseline AOD_{750} ≤300 µm showed nearly 96% sensitivity and 65% specificity in identifying individuals at risk of incident angle closure at 4-year follow-up.[7,37,58]

The trabecular-iris angle, commonly referenced at 500 µm from the SS (TIA_{500}), is a measure of the angle in degrees between the 2 lines connecting the deepest part of the angle recess and the ends of the line representing the AOD_{500}. The smaller the AOD_{500}, the narrower the TIA_{500}.[59]

Defined as the triangular area between the anterior iris surface, the posterior corneoscleral surface, and the AOD, measured in µm, ARA is smaller in individuals with angle closure and increases following LPI.[5,53,60]

Effectively representing a portion of the ARA, the trabecular-iris space area (TISA) is also smaller in individuals who progress from PACS to PAC and increases following LPI.[4,5,53,58] TISA is defined as the trapezoidal area bounded by the AOD (at 500 or 750 µm) anteriorly, a line between the SS and

Figure 2. A diagram representing the relationship between angle opening distance (AOD_{500}, on left), trabecular-iris angle (TIA_{500}, in centre), and trabecular-iris space area ($TISA_{500}$, on right)

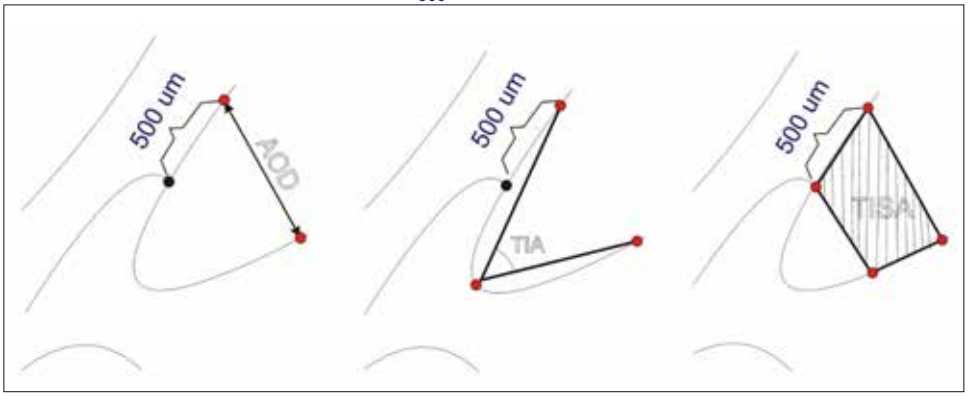

The AOD, TIA, and TISA are all dependent on accurate and precise localization of the scleral spur.

Figure 3. Despite having fairly symmetric angle opening distance (AOD_{750}), the temporal angle (on left) has a smaller angle recess area (ARA_{750}) than the nasal angle (on right), putting it at higher risk of closure

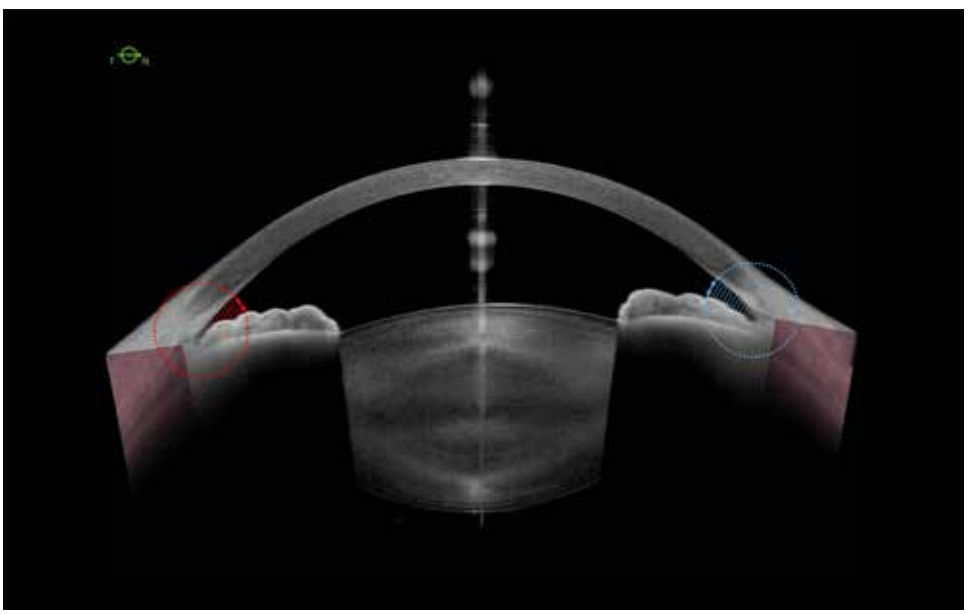

anterior iris perpendicular to the scleral wall posteriorly, the corneoscleral surface superiorly, and the anterior iris surface inferiorly.

The relationship between AOD_{500}, TIA_{500}, and $TISA_{500}$ is shown diagrammatically in Figure 2.[61]

Refer to Figure 3 for an example of the influence of peripheral iris contour on risk of angle closure. Note that despite fairly symmetric AOD_{750}, the temporal angle (on the left in this image) has a significantly smaller ARA_{750}, putting it at higher risk of closure.

Figure 4. Post-cataract or clear lens extraction

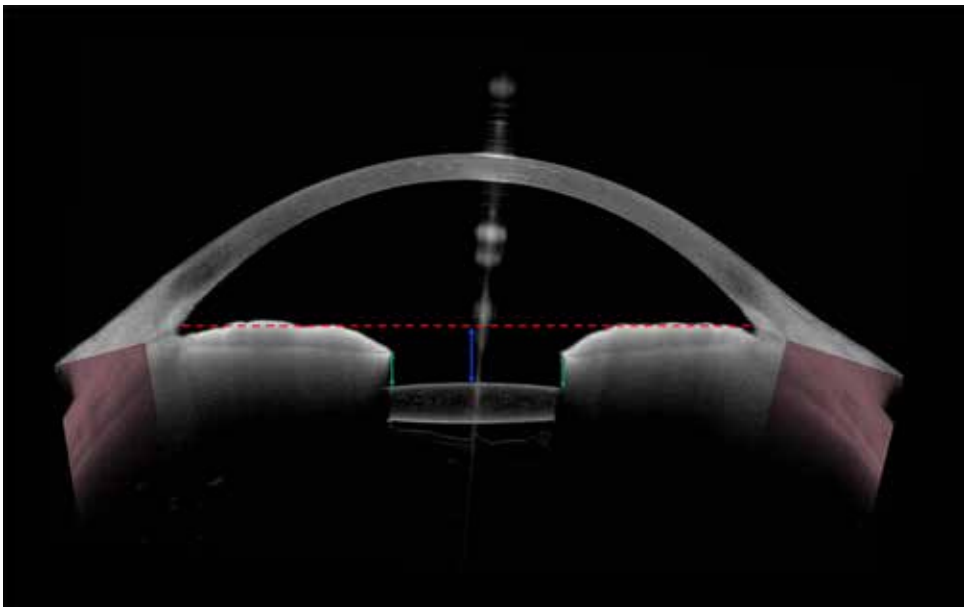

Note the presence of negative lens vault (blue arrow) and absence of irido-lenticular/irido-intraocular lens implant touch (green arrows) even though the iris margin is more posterior than its root.

Given that the SS can be difficult to visualize in nearly 1 in 4 eyes, the measurement of AOD at the level of Schwalbe's line (AOD_{SL}) has been proposed as an alternative to metrics referenced to the SS.[62] The AOD_{SL} is the distance between SL (visible in >95% of eyes as the inner junction between darker corneal stroma and brighter sclera at the limbus; refer to Figure 1) and the iris surface perpendicular to the corneal endothelium. In fact, given that the length of the TM shows significant inter-individual variability and may be shorter in individuals with angle-closure glaucoma than those without,[63] AOD_{SL} may be a better measure of whether aqueous is able to access the TM than AOD_{500} or AOD_{750}.

Using SL as the landmark, trabecular-iris space area at the level of Schwalbe's line ($TISA_{SL}$) may be calculated as the trapezoidal area bounded by the AOD_{SL} anteriorly, a line between the scleral wall and anterior iris drawn perpendicular to the scleral wall an arbitrary 500 µm posterior to the SL, the corneoscleral surface superiorly, and the anterior iris surface inferiorly.[64] The ability of $TISA_{SL}$ to identify angle closure has proven comparable to gonioscopy and both $TISA_{500}$ and $TISA_{750}$, again with the advantage of SL being more readily identifiable than SS in most SD-OCT images. Moreover, by accounting for iris curvature posterior to the level of SL (refer to Figure 3), $TISA_{SL}$ may reflect angle anatomy and the attendant risk of closure more accurately than AOD_{SL}.[64]

Lens vault (LV) is defined as the perpendicular distance between the anterior lens surface and a horizontal line connecting the opposing SS (a proxy for the posterior limit of the angle).[9,65] LV quantifies the amount of crystalline lens in the anterior part of the eye and is one of the strongest contributors to reduced angle width. Baseline LV >0.56 mm was nearly 65% sensitive and 84% specific in identifying individuals who went on to develop angle closure at 4-year follow-up.[58]

Eyes with PACG have significantly greater LV than do healthy eyes (1.06 vs. 0.36 mm),[66] and individuals in the quartile with the greatest LV are nearly 50 times more likely to have PAC than those in the quartile with the lowest.[9] Mechanistically, greater LV

Figure 5. A swept-source anterior segment optical coherence tomography image depicting numerous anterior segment parameters

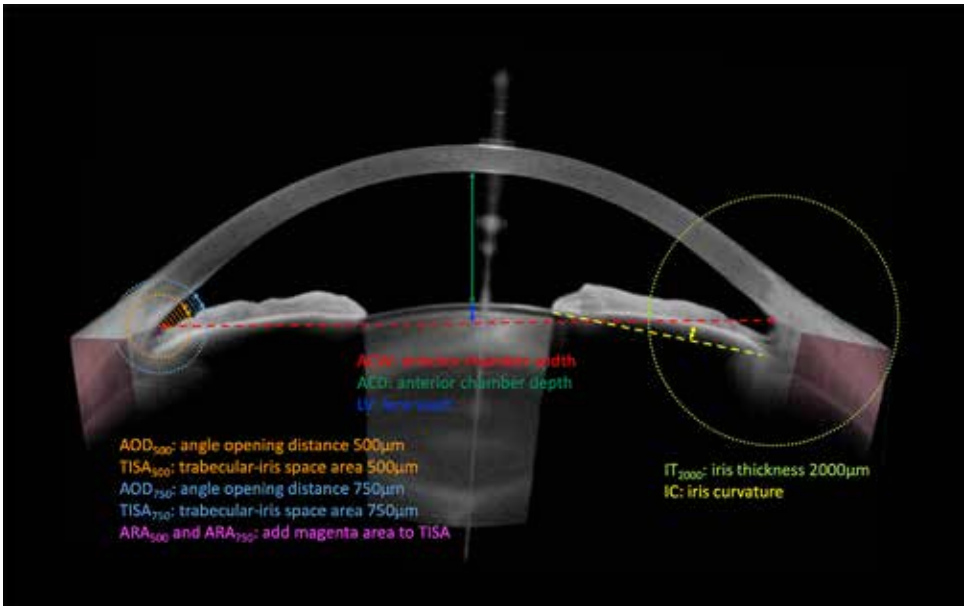

Parameters include anterior chamber width (ACW) and anterior chamber depth (ACD), lens vault (LV), angle opening distance (AOD), trabecular-iris space area (TISA), angle recess area (ARA), iris curvature (IC), and iris thickness (IT), many of which are dependent on accurate and precise localization of the scleral spur. Anterior chamber area is bound by the posterior cornea, anterior iris, and anterior lens surface. Anterior chamber volume is calculated by rotating ACA 360° around a vertical axis through its midpoint.

forces the iris more anteriorly, potentially strengthening pupillary block and increasing risk of ITC and incident angle-closure disease, independent of lens thickness and ACD.[53,65]

On AS-OCT imaging of eyes with greater LV, the iris appears to drape over a large portion of the anterior surface of the lens, what some have characterized as a volcano-like configuration.[67]

LV tends to increase with advancing cataract, may decrease after LPI (further reducing the risk of persistent pupillary block), and definitely decreases after cataract or clear lens extraction (refer to Figure 4).[9,28,68] Not surprisingly, patients with pronounced LV tend to experience significant intraocular pressure decrease following lens extraction.[67]

The importance of LV was alluded to in the late 1990s, well before AS-OCT was on the scene, when Salmon opined that "the most important biometric feature predisposing to angle-closure glaucoma is the relative forward position of the anterior lens surface in relation to the iris root."[69]

Iris curvature (IC) is increased in the presence of pupillary block (reflecting iris bombe), and flattens following LPI, contributing to an increase in ACA and ACV.[6,53,70] IC is defined as the perpendicular distance in millimetres between the posterior iris surface at its point of greatest curvature and the 2 points marking the most peripheral and most central iris pigment epithelium.

Greater AS-OCT quantified IC, iris area, and iris thickness all crowd the angle and have proven to independently increase the odds of an angle being narrow by 2.5 to 2.7 times.[7,9,71] Iris area is the cumulative cross-sectional area of the iris from SS to pupil

margin. Iris thickness is measured at a fixed distance from the SS (commonly 750 and 2,000 µm) or iris root (commonly 500 and 1,000 µm).

Further, increased peripheral iris thickness is more commonly found in individuals over the age of 65 years, Asian individuals, and those with a history of PACG.[4,72]

Retrospective analysis of Zhongshan Angle Closure Prevention Trial data identified smaller angle width (narrow horizontal AOD_{500} and horizontal $TISA_{500}$ ≤0.05 mm^2) and cumulative gonioscopy score ≤6 at two weeks post-LPI as biometric risk factors predictive of progression in LPI-treated PACS eyes.[73] The cumulative gonioscopy score is the sum of four quadrants of gonioscopic grades, where grade 0 is no structures visible, grade 2 is posterior TM visible, and grade 4 is CB visible. This confirmed that the protective effect of LPI was strongly driven by angle widening and suggests that AS-OCT may be of more predictive value in eyes with narrower pre-LPI angles, while gonioscopy may be more helpful in eyes with wider (or more variable) post-LPI configurations. These data also emphasized the importance of careful angle assessment following LPI, ideally leveraging both quantitative (AS-OCT) and qualitative (gonioscopic) testing, to better identify eyes at higher risk of post-LPI progression and inform individualized follow-up.[74]

A representative swept-source AS-OCT image depicting ACW, ACD, LV, AOD, TISA, ARA, IC, and iris thickness is presented as Figure 5.

Although static biometric (or anatomic) parameters account for a great deal of the variability in angle width, dynamic (or physiologic) changes in the iris and choroid also play important roles.[34,72] This is highlighted by the fact that despite comparable anterior segment anatomy, Asian eyes have a 5-fold greater risk of PACG than do European eyes.[75]

As an example, whereas iris volume tends to decrease with mydriasis in controls, it has been shown to decrease less (or in some cases increase) in individuals with angle closure, creating ITC and physically obstructing the TM.[76,77] It has been hypothesized that iris density is increased and fluid conductivity is impaired in eyes of individuals over the age of 65 years, those with a history of acute primary angle closure (APAC), and those with fewer radial iris crypts and more concentric iris furrows.[72] In fact, the odds of APAC were nearly 9 times higher in eyes with no iris crypts than in those with numerous crypts.[78]

Moving more posteriorly, choroidal expansion/effusion (abnormal accumulation of fluid in the suprachoroidal space, best visualized with UBM) in the relatively rigid corneoscleral shell may cause an anterior displacement of the vitreous, lens, and iris. This can narrow the angle and precipitate APAC, particularly in smaller hyperopic eyes with already narrow angles and increased resistance to fluid flow through the anterior vitreous.[23,79-81] This mechanism may be contributory to some presentations of iatrogenic (medication-induced) APAC reviewed earlier, including that secondary to topiramate.[82]

Conclusion

PACG remains an important yet unfortunately and unnecessarily an under-diagnosed cause of glaucoma-related visual impairment. Through recognition of risk factors, careful clinical assessment, and the judicious use of evolving ancillary imaging modalities, primary care optometrists can identify this largely preventable disease of ocular anatomy early in the angle-closure spectrum. This sets the stage for effective medical, procedural, and surgical intervention, means to the end of preventing vision loss and preserving vision-related quality of life.

Disclosures

Funding: This study did not receive any specific grant from funding agencies in the public, commercial, or not-for-profit sectors.

Competing interests: All authors have completed the ICMJE uniform disclosure form and declare no conflict of interest.

Artificial intelligence statement: The authors confirm no generative AI or AI-assisted technology was used to generate content.

Corresponding author: Derek MacDonald, derek.macdonald.ilexeye@gmail.com

References

1. Pinto LA. (2021). *Time to refine your glaucoma practice*. Nidek Experience Center.
2. Riva I, Micheletti E, Oddone F, et al. Anterior chamber angle assessment techniques: A review. *J Clin Med.* 2020;9(12):3814. https://doi.org/10.3390/jcm9123814
3. Teixeira F, Sousa DC, Leal I, Barata A, Neves CM, Pinto LA. Automated gonioscopy photography for iridocorneal angle grading. *Eur J Ophthalmol.* 2020;30(1):112-118. https://doi.org/10.1177/1120672118806436
4. Xu BY, Friedman DS, Foster PJ, et al. Ocular biometric risk factors for progression of primary angle closure disease. The Zhongshan Angle Closure Prevention Trial. *Ophthalmology*. 2022;129(3):267-275. https://doi.org/10.1016/j.ophtha.2021.10.003
5. Radhakrishnan S, See J, Smith SD, et al. Reproducibility of anterior chamber angle measurements obtained with anterior segment optical coherence tomography. *Invest Ophthalmol Vis Sci.* 2007;48(8):3683-3688. https://doi.org/10.1167/iovs.06-1120
6. Jiang Y, Chang DS, Zhu H, et al. Longitudinal changes of angle configuration in primary angle-closure suspects. The Zhongshan Angle-Closure Prevention Trial. *Ophthalmology*. 2014;121(9):1699-1705. https://doi.org/10.1016/j.ophtha.2014.03.039
7. Nongpiur ME, Ku JY, Aung T. Angle closure glaucoma: A mechanistic review. *Curr Opin Ophthalmol.* 2011;22(2):96-101. https://doi.org/10.1097/ICU.0b013e32834372b9
8. He M, Foster PJ, Johnson GJ, Khaw PT. Angle-closure glaucoma in East Asian and European people: Different diseases? *Eye*. 2006;20(1):3-12. https://doi.org/10.1038/sj.eye.6701797
9. Nongpiur ME, He M, Amerasinghe N, et al. Lens vault, thickness and position in Chinese subjects with angle closure. *Ophthalmology*. 2011;118(3):474-479. https://doi.org/10.1016/j.ophtha.2010.07.025
10. Leung CK-S, Weinreb RN. Anterior chamber imaging with optical coherence tomography. *Eye*. 2011;25(3):261-267. https://doi.org/10.1038/eye.2010.201
11. Pavlin CJ, Ritch R, Foster FS. Ultrasound biomicroscopy in plateau iris syndrome. *Am J Ophthalmol*. 1992;113(4):390-395. https://doi.org/10.1016/s0002-9394(14)76160-4
12. Smith SD, Singh K, Lin SC, et al. Evaluation of the anterior chamber angle in glaucoma: A report by the American Academy of Ophthalmology. *Ophthalmology*. 2013;120(10):1985-1997. https://doi.org/10.1016/j.ophtha.2013.05.034
13. Barkana Y, Dorairaj SK, Gerber Y, Liebmann JM, Ritch R. Agreement between gonioscopy and ultrasound biomicroscopy in detecting iridotrabecular apposition. *Arch Ophthalmol.* 2007;125(10):1331-1335. https://doi.org/10.1001/archopht.125.10.1331
14. Kong X, Foster PJ, Huang Q, et al. Appositional closure identified by ultrasound biomicroscopy in population-based primary angle-closure glaucoma suspects: The Liwan Eye Study. *Invest Ophthalmol Vis Sci.* 2011;52(7):3970-3975. https://doi.org/10.1167/iovs.10-6412
15. Radhakrishnan S, Chen L. Diagnosis and monitoring of primary angle closure. *Curr Ophthalmol Rep.* 2015;3:51-57. https://doi.org/10.1007/s40135-015-0063-y
16. Xu Y, Tan Q, Li C, Liu D. The ocular biometry characteristics of young patients with primary angle-closure glaucoma. *BMC Ophthalmol.* 2022;22(1):150. https://doi.org/10.1186/s12886-022-02374-2
17. Gazzard G, Friedman DS, Devereux JG, Chew P, Seah SK. A prospective ultrasound biomicroscopy evaluation of changes in anterior segment morphology after laser iridotomy in Asian eyes. *Ophthalmology*. 2003;110(3):630-638. https://doi.org/10.1016/S0161-6420(02)01893-6
18. Jones LW, Srinivasan S, Ng A, Schulz Me. (2018). Diagnostic instruments. In N. Efron (Ed.), *Contact Lens Practice* (3rd ed., 327-345). Elsevier.
19. Rabsilber TM, Khoramnia R, Auffarth GU. Anterior chamber measurements using Pentacam rotating Scheimpflug camera. *J Cataract Refract Surg*. 2006;32(3):456-459. https://doi.org/10.1016/j.jcrs.2005.12.103
20. Rodrigues EB, Johanson M, Penha FM. Anterior segment tomography with the Cirrus optical coherence tomography. *J Ophthalmol*. 2012:806989. https://doi.org/10.1155/2012/806989
21. Kurita N, Mayama C, Tomidokoro A, Aihara M, Araie M. Potential of the Pentacam in screening

for primary angle closure and primary angle closure suspect. *J Glaucoma.* 2009;18(7):506-512. https://doi.org/10.1097/IJG.0b013e318193c141

22. Huang D, Swanson EA, Lin CP, et al. Optical coherence tomography. *Science*. 1991;254(5035):1178-1181. https://doi.org/10.1126/science.1957169
23. Sun X, Dai Y, Chen Y, et al. Primary angle closure glaucoma: What we know and what we don't know. *Prog Ret Eye Res.* 2017;57:26-45. https://doi.org/10.1016/j.preteyeres.2016.12.003
24. Prata TS, Dorairaj S, De Moraes CG, Tello C, Liebmann JM, Ritch R. Indentation slit lamp-adapted optical coherence tomography technique for anterior chamber angle assessment. *Arch Ophthalmol.* 2010;128(5):646-647. https://doi.org/10.1001/archophthalmol.2010.51
25. Marion KM, Dastiridou A, Niemeyer M, Francis BA, Sadda SR, Chopra V. Anterior chamber angle morphometry measurement changes to ambient illumination scaling in Visante time domain optical coherence tomography. *Curr Eye Res.* 2017;42(3):386-393. https://doi.org/10.1080/02713683.2016.1190847
26. Lai I, Mak H, Lai G, Yu M, Lam DS, Leung CK. Anterior chamber angle imaging with swept-source optical coherence tomography: Measuring peripheral anterior synechia in glaucoma. *Ophthalmology*. 2013;120(6):1144-1149. https://doi.org/10.1016/j.ophtha.2012.12.006
27. Tun TA, Baskaran M, Tan SS, Perera SA, Aung T, Husain R. Evaluation of the anterior segment angle-to-angle scan of Cirrus High-Definition Optical Coherence Tomography and comparison with gonioscopy and with the Visante OCT. *Invest Ophthalmol Vis Sci.* 2017;58(1):59-64. https://doi.org/10.1167/iovs.16-20886
28. Selvan H, Angmo D, Tomar AS, Yadav S, Sharma A, Dada T. Changes in intraocular pressure and angle status after phacoemulsification in primary angle closure hypertension. *J Glaucoma.* 2019;28(2):105-110. https://doi.org/10.1097/IJG.0000000000001137
29. Xie Q, Ma P, Patlidanon J, et al. Anterior segment OCT in primary angle closure disease compared with normal subjects with similar shallow anterior chamber. *J Glaucoma*. 2022;31(2):84-90. https://doi.org/10.1097/IJG.0000000000001915
30. Maslin JS, Barkana Y, Dorairaj SK. Anterior segment imaging in glaucoma: An updated review. *Indian J Ophthalmol*. 2015;63(8):630-640. https://doi.org/10.4103/0301-4738.169787
31. Angmo D, Nongpiur ME, Sharma R, Sidhu T, Sihota R, Dada T. Clinical utility of anterior segment swept-source optical coherence tomography in glaucoma. *Oman J Ophthalmol.* 2016;9(1):3-10. https://doi.org/10.4103/0974-620X.176093
32. Sakata LM, Lavanya R, Friedman DS, et al. Assessment of the scleral spur in anterior segment optical coherence tomography images. *Arch Ophthalmol*. 2008;126(2):181-185. https://doi.org/10.1001/archophthalmol.2007.46
33. Seager FE, Wang J, Arora KS, Quigley HA. The effect of scleral spur identification methods on structural measurements by anterior segment optical coherence tomography. *J Glaucoma.* 2014;23(1):e29-e38. https://doi.org/10.1097/IJG.0b013e31829e55ae
34. Foo LL, Nongpiur ME, Allen JC, et al. Determinants of angle width in Chinese Singaporeans. *Ophthalmology*. 2012;119(2):278-282. https://doi.org/10.1016/j.ophtha.2011.07.049
35. Porporato N, Baskaran M, Aung T. Role of anterior segment optical coherence tomography in angle-closure disease: A review. *Clin Exp Ophthalmol.* 2018;46(2):147-157. https://doi.org/10.1111/ceo.13120
36. Console JW, Sakata LM, Aung T, Friedman DS, He M. Quantitative analysis of anterior segment optical coherence tomography images: the Zhongshan Angle Assessment Program. *Br J Ophthalmol.* 2008;92(12):1612-1616. https://doi.org/10.1136/bjo.2007.129932
37. Narayanaswamy A, Sakata LM, He MG, et al. Diagnostic performance of anterior chamber angle measurements for detecting eyes with narrow angles: an anterior segment OCT study. *Arch Ophthalmol.* 2010;128(10):1321-1327. https://doi.org/10.1001/archophthalmol.2010.231
38. Zhao Y, Chen J, Yu X, Xu J, Sun X, Hong J. Age-related changed in human Schlemm's canal: an in vivo optical coherence tomography-based study. *Front Physiol.* 2018;9:630. https://doi.org/10.3389/fphys.2018.00630
39. Wong HT, Lim MC, Sakata LM, et al. High-definition optical coherence tomography imaging of the iridocorneal angle of the eye. *Arch Ophthalmol.*

2009;127(3):256-260. https://doi.org/10.1001/archophthalmol.2009.22

40. Crowell EL, Baker L, Chuang AZ, et al. Characterizing anterior segment OCT angle landmarks of the trabecular meshwork complex. *Ophthalmology*. 2018;125(7):994-1002. https://doi.org/10.1016/j.ophtha.2018.01.018
41. Fukuda S, Kawana K, Yasuno Y, Oshika T. Anterior ocular biometry using 3-dimensional optical coherence tomography. *Ophthalmology*. 2009;116(5):882-889. https://doi.org/10.1016/j.ophtha.2008.12.022
42. Gora M, Karnowski K, Szkulmowski M, et al. Ultra high-speed swept source OCT imaging of the anterior segment of the human eye at 200kHz with an adjustable image range. *Optics Express.* 2009;17(17):14880-14894. https://doi.org/10.1364/oe.17.014880
43. Chan PP, Lai G, Chiu V, Chong A, Yu M, Leung CK. Anterior chamber angle imaging with swept-source optical coherence tomography: Comparison between CASIAII and ANTERION. *Sci Rep*. 2020;10(1):18771. https://doi.org/10.1038/s41598-020-74813-3
44. Chen X, Wang X, Tang Y, Sun X, Chen Y. Optical coherence tomography analysis of anterior segment parameters before and after laser peripheral iridotomy in primary angle-closure suspects using CASIA2. *BMC Ophthalmol.* 2022;22(1):144. https://doi.org/10.1186/s12886-022-02366-2
45. Fernández-Vigo JI, Kudsieh B, Shi H, De-Pablo-Gómez-de-Liaño L, Fernández-Vigo JÁ, García-Feijóo J. Diagnostic imaging of the ciliary body: technologies, outcomes, and future perspectives. *Eur J Ophthalmol*. 2022;32(1):75-88. https://doi.org/10.1177/11206721211031409
46. Lai I, Mak H, Lai G, Yu M, Lam DS, Leung CK. Anterior chamber angle imaging with swept-source optical coherence tomography: Measuring peripheral anterior synechia in glaucoma. *Ophthalmology*. 2013;120(6):1144-1149. https://doi.org/10.1016/j.ophtha.2012.12.006
47. Radhakrishnan S, Goldsmith J, Huang D, et al. Comparison of optical coherence tomography and ultrasound biomicroscopy for detection of narrow anterior chamber angles. *Arch Ophthalmol*. 2005;123(8):1053-1059. https://doi.org/10.1001/archopht.123.8.1053
48 Nolan WP, See JL, Chew PT, et al. Detection of primary angle closure using anterior segment optical coherence tomography in Asian eyes. *Ophthalmology*. 2007;114(1):33-39. https://doi.org/10.1016/j.ophtha.2006.05.073
49. Xu BY, Pardeshi AA, Burkemper B, et al. Differences in anterior chamber angle assessment between gonioscopy, Eyecam, and anterior segment OCT: the Chinese American Eye Study. *Trans Vis Sci Technol.* 2019;8(2):5. https://doi.org/10.1167/tvst.8.2.5
50. Porporato N, Baskaran M, Tun TA, et al. Understanding diagnostic disagreement in angle closure assessment between anterior segment optical coherence tomography and gonioscopy. *Br J Ophthalmol.* 2020;104(6):795-799. https://doi.org/10.1136/bjophthalmol-2019-314672
51. Baskaran M, Iyer JV, Narayanaswamy AK, et al. Anterior segment imaging predicts incident gonioscopic angle closure. *Ophthalmology*. 2015;122(12):2380-2384. https://doi.org/10.1016/j.ophtha.2015.07.030
52. Zhang X, Guo PY, Lin C, et al. Assessment of iris trabecular contact in eyes with gonioscopic angleclosure. *Ophthalmology*. 2022;130(1):111-119. https://doi.org/doi:10.1016/j.ophtha.2022.08.017
53. How AC, Baskaran M, Kumar RS, et al. Changes in anterior segment morphology after laser peripheral iridotomy: An anterior segment optical coherence tomography study. *Ophthalmology*. 2012;119(7):1383-1387. https://doi.org/10.1016/j.ophtha.2012.01.019
54. Nongpiur ME, Sakata LM, Friedman DS, et al. Novel association of smaller anterior chamber width with angle closure in Singaporeans. *Ophthalmology*. 2010;117(10):1967-1973. https://doi.org/10.1016/j.ophtha.2010.02.007
55. Wu RY, Nongpiur ME, He MG, et al. Association of narrow angles with anterior chamber area and volume measured with anterior segment optical coherence tomography. *Arch Ophthalmol.* 2011;129(5):569-574. https://doi.org/10.1001/archophthalmol.2011.68
56. Fontana ST, Brubaker FR. Volume and depth of the anterior chamber in the normal aging human eye. *Arch Ophthalmol.* 1980;98(10):1803-1808. https://doi.org/10.1001/archopht.1980.01020040655013

57. Sun JH, Sung KR, Yun SC, et al. Factors associated with anterior chamber narrowing with age: an optical coherence tomography study. *Invest Ophthalmol Vis Sci.* 2012;53(6):2607-2610. https://doi.org/10.1167/iovs.11-9359
58. Nongpiur ME, Aboobakar IF, Baskaran M, et al. Association of baseline anterior segment parameters with the development of incident gonioscopic angle closure. *JAMA Ophthalmol.* 2017;135(3):252-258. https://doi.org/10.1001/jamaophthalmol.2016.5847
59. Ghadamzadeh M, Karimi F, Ghasemi Moghaddam S, Daneshvar R. Anterior chamber angle changes in primary angle-closure glaucoma following phacoemulsification versus phacotrabeculectomy: A prospective randomized clinical trial. *J Glaucoma.* 2022;31(3):147-155. https://doi.org/10.1097/IJG.0000000000001977
60. Ishikawa H, Esaki K, Liebmann JM, Uji Y, Ritch R. Ultrasound biomicroscopy dark room provocative testing: a quantitative method for estimating anterior chamber angle width. *Jpn J Ophthalmol.* 1999;43(6):526-534. https://doi.org/10.1016/s0021-5155(99)00139-2
61. Koprowski R, Wróbel Z. *Image Processing in Optical Coherence Tomography: Using Matlab.* Katowice (Poland): University of Silesia; 2011.
62. Qin B, Francis BA, Li Y, et al. Anterior chamber angle measurements using Schwalbe's line with high-resolution Fourier-domain optical coherence tomography. *J Glaucoma.* 2013;22(9):684-288. https://doi.org/10.1097/IJG.0b013e318264b921
63. Masis Solano M, Lin SC. Cataract, phacoemulsification and intraocular pressure: is the anterior segment anatomy the missing piece of the puzzle? *Prog Ret Eye Res.* 2018;64:77-83. https://doi.org/10.1016/j.preteyeres.2018.01.003
64. Cheung CY, Zheng C, Ho CL, et al. Novel anterior-chamber angle measurements by high-definition optical coherence tomography using the Schwalbe line as the landmark. *Br J Ophthalmol.* 2011;95(7):955-959. https://doi.org/10.1136/bjo.2010.189217
65. Ozaki M, Nongpiur ME, Aung T, He M, Mizoguchi T. Increased lens vault as a risk factor for angle closure: confirmation in a Japanese population. *Graefes Arch Clin Exp Ophthalmol.* 2012;250(12):1863-1868. https://doi.org/10.1007/s00417-012-2011-y
66. Kim YK, Yoo BW, Kim HC, Aung T, Park KH. Relative lens vault in subjects with angle closure. *BMC Ophthalmol.* 2014;14:93. https://doi.org/10.1186/1471-2415-14-93
67. Song MK, Sung KR, Shin JW. Glaucoma progression after lens extraction in primary angle-closure glaucoma according to angle-closure mechanism. *J Glaucoma.* 2022;31(4):261-267. https://doi.org/10.1097/IJG.0000000000001992
68. Koh V, Keshtkaran MR, Hernstadt D, Aquino MCD, Chew PT, Sng C. Predicting the outcome of laser peripheral iridotomy for primary angle closure suspect eyes using anterior segment optical coherence tomography. *Acta Ophthalmol.* 2019;97(1):e57-e63. https://doi.org/10.1111/aos.13822
69. Salmon JF. Predisposing factors for chronic angle-closure glaucoma. *Prog Ret Eye Res.* 1999;18(1):121-132. https://doi.org/10.1016/s1350-9462(98)00007-x
70. Xu BY, Friedman DS, Foster PJ, et al. Anatomic changes and predictors of angle widening after laser peripheral iridotomy. The Zhongshan Angle Closure Prevention Trial. *Ophthalmology*. 2021;128(8):1161-1168. https://doi.org/10.1016/j.ophtha.2021.01.021
71. Wang BS, Sakata LM, Friedman DS, et al. Quantitative iris parameters and association with narrow angles. *Ophthalmology*. 2010;117(1):11-17. https://doi.org/10.1016/j.ophtha.2009.06.017
72. Soh ZD, Thakur S, Majithia S, Nongpiur ME, Cheng CY. Iris and its relevance to angle closure disease: A review. *Br J Ophthalmol.* 2021;105(1):3-8. https://doi.org/10.1136/bjophthalmol-2020-316075
73. Bao YK, Xu BY, Friedman DS, et al. Biometric risk factors for angle closure progression after laser peripheral iridotomy. *JAMA Ophthalmol.* 2023;141(6):516-524. https://doi.org/10.1001/jamaophthalmol.2023.0937
74. Azuara-Blanco A. Use of biometric data after laser peripheral iridotomy – individualized monitoring strategy for angle closure prevention. *JAMA Ophthalmol.* 2023;141(6):524. https://doi.org/10.1001/jamaophthalmol.2023.1119
75. Congdon NG, Youlin Q, Quigley H, et al. Biometry and primary angle-closure glaucoma among Chinese, white and black populations. *Ophthalmology*. 1997;104(9):1489-1495. https://doi.org/10.1016/s0161-6420(97)30112-2

76. Quigley HA, Silver DM, Friedman DS, et al. Iris cross-sectional area decreases with pupil dilation and its dynamic behavior is a risk factor in angle closure. *J Glaucoma*. 2009;18(3):173-179. https://doi.org/10.1097/IJG.0b013e31818624ce

77. Aptel F, Denis P. Optical coherence tomography quantitative analysis of iris volume changes after pharmacologic mydriasis. *Ophthalmology*. 2010;117(1):3-10. https://doi.org/10.1016/j.ophtha.2009.10.030

78. Koh V, Chua J, Shi Y, et al. Association of iris crypts with acute primary angle closure. *Br J Ophthalmol.* 2017;101(10):1318-1322. https://doi.org/10.1136/bjophthalmol-2016-309842

79. Quigley HA, Friedman DS, Congdon NG. Possible mechanisms of primary angle-closure and malignant glaucoma. *J Glaucoma*. 2003;12(2):167-180. https://doi.org/10.1097/00061198-200304000-00013

80. Sakai H, Morine-Shinjyo S, Shinzato M, Nakamura Y, Sakai M, Sawaguchi S. Uveal effusion in primary angle-closure glaucoma. *Ophthalmology*. 2005;112(3):413-419. https://doi.org/10.1016/j.ophtha.2004.08.026

81. Kumar RS, Baskaran M, Chew PT, et al. Prevalence of plateau iris in primary angle closure suspects: an ultrasound biomicroscopy study. *Ophthalmology*. 2008;115(3):430-434. https://doi.org/10.1016/j.ophtha.2007.07.026

82. Na KI, Park SP. Association of drugs with angle closure. *JAMA* Ophthalmol. 2022;140(11):1055-1063. https://doi.org/10.1001/jamaophthalmol.2022.3723